

Compression and Parametric Driving of Atoms in Optical Lattices

G. Raithel, G. Birkl,* W. D. Phillips, and S. L. Rolston

National Institute of Standards and Technology, PHYS A167, Gaithersburg, Maryland 20899

(Received 9 September 1996)

Using Bragg scattering we study classical squeezing and wave packet oscillations of the atomic center-of-mass motion of cesium atoms trapped in 1D and 3D optical lattices. A sudden increase of the potential depth leads to wave packets substantially more localized than in steady state, and subsequent breathing-mode oscillations with a decay rate that under some conditions is remarkably slow. We also study the response of the atoms to parametric driving of the center-of-mass motion. Our results are in agreement with Monte Carlo simulations. [S0031-9007(97)02911-6]

PACS numbers: 32.80.Lg, 32.80.Pj, 42.50.Vk

Optical lattices are periodic light-shift potentials for atoms, created by the interference of multiple laser beams. The steady state properties of atoms trapped in lattices have recently been extensively investigated [1–3]. Such lattices offer an interesting model system for solid state physics, with completely characterized potentials, and the ability to manipulate the potentials. Recent observations of Bloch oscillations [4] and the Wannier-Stark ladder [5] for atoms trapped in optical lattices are examples. In this work we create breathing-mode atomic wave packets by modulating the potentials, either by sudden changes in the potential depth or by parametric driving. We measure this wave packet motion using Bragg scattering, a sensitive probe for the atomic localization [6–8]. Study of the wave packet dynamics not only yields information about the coherent and incoherent components of the atomic motion, but also allows exploration of the quantum phenomenon of revivals, due to the anharmonic character of the potentials, and the creation of superlocalized wave packets, whose rms spread is substantially below the steady state value.

By changing the intensity of the light forming the lattice, we manipulate the potential. A sudden increase of intensity deepens the light-shift potential wells, causing a compression of the atomic spatial distribution, followed by a damped, oscillatory, wave packet motion. This method of wave packet excitation has the advantage of producing transient compression of the atomic probability distribution to as small as a few tens of nanometers for a duration of a few microseconds. Using periodic modulation of the potential depth to parametrically drive the system, we can also generate periodic wave packet oscillations.

As in [7] we measure the mean-square displacement $\Delta\xi^2$ of the atoms from the lattice sites in the direction of the momentum transfer $\hbar\mathbf{K}$ associated with the Bragg reflection. Since the Bragg reflectivity is proportional to the Debye-Waller factor $\exp(-K^2 \Delta\xi^2)$,

$$\Delta\xi^2(t) = -\frac{\ln[I_B(t)/I_B(\infty)]}{K^2} + \Delta\xi^2(\infty), \quad (1)$$

where I_B is the measured Bragg reflectivity. We performed experiments with a 1D and a 3D optical lattice, for

which $K = 4\pi/\lambda$ and $K = 2\sqrt{2}\pi/\lambda$, respectively [7]. At long times $\Delta\xi^2$ approaches the known steady state values, $\Delta\xi^2(\infty) = (\lambda/7.3)^2$ in 3D and $\Delta\xi^2(\infty) = (\lambda/18)^2$ in 1D, as measured in [9], nearly independent of intensity and detuning.

The experimental setup has been described previously [6]. Cesium atoms are collected, cooled, and trapped on the $6S_{1/2}, F=4 \rightarrow 6P_{3/2}, F=5$ transition ($\Gamma/2\pi = 5.2$ MHz; $\lambda = 2\pi/k = 852$ nm; $2E_R/k_B = \hbar^2 k^2/mk_B = 200$ nK). We investigate the 1D lin \perp lin lattice configuration [1] as well as its 3D generalization, consisting of two pairs of laser beams linearly polarized along x and y , as used in Ref. [6]. In 1D the light-shift potential wells are spaced by $\lambda/4$; in 3D they are spaced by $\lambda/(2\sqrt{2})$ along z , and $\lambda/\sqrt{2}$ along x and y . Atoms are trapped, cooled, and allowed to reach the steady state localization $\Delta\xi^2(\infty)$ while the lattice light intensity is held constant at an initial value. We then compress or parametrically drive the localized atoms by suddenly increasing the lattice intensity or sinusoidally modulating it about its initial value. After a variable time interval, the light is turned off and with a delay of $\approx 0.2 \mu\text{s}$ a weak probe pulse measuring the Bragg reflectivity of the sample is introduced [6]. We obtain $\Delta\xi^2(t)$ from the measured Bragg reflectivity, using Eq. (1).

When the potential depth is changed at $t = 0$ from U_{initial} to U_{final} within a time interval short compared to the vibrational period of the atoms [10], we observe wave packet compression and breathing-mode oscillations with half the vibrational period of the atoms in the potential wells. Quantum mechanically, the symmetric excitation creates coherences between vibrational levels with quantum numbers differing by two. Figure 1 shows a typical 3D result. In the harmonic approximation the compression $C(t) = \sqrt{\Delta\xi^2(0)/\Delta\xi^2(t)}$ reaches its maximum value, $\sqrt{U_{\text{final}}/U_{\text{initial}}}$, at about a quarter of the vibrational period after the switching [10] [since we start in steady state, $\Delta\xi^2(0) = \Delta\xi^2(\infty)$]. A maximum compression $C \approx 2$ is observed, corresponding to the minimum in Fig. 1, as expected for the parameters used.

For a harmonic well and no damping, $\Delta\xi^2(t)$ would oscillate between $\Delta\xi^2(0)$ and its minimum value given

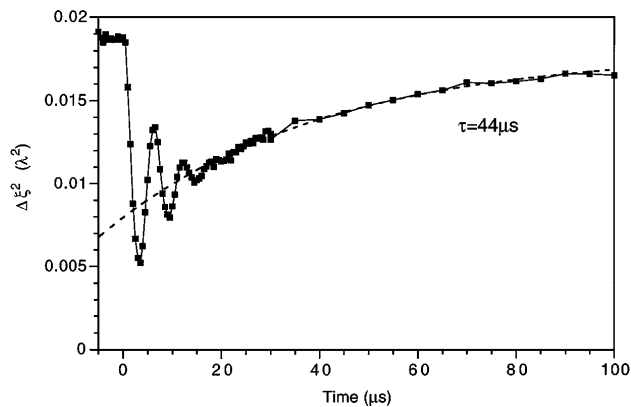


FIG. 1. Wave packet oscillation of the mean square position spread in a 3D optical lattice ($\delta = -5\Gamma$) induced by a sudden increase of the potential depth from $850E_R$ to $3170E_R$ at $t = 0$. The vibrational period of the atoms in the lattice for $t > 0$ is $\approx 10 \mu\text{s}$. The long-term exponential approach to steady state (heating) is best fitted with a time-constant of $44 \mu\text{s}$ (dashed line).

by $\Delta\xi^2(0) U_{\text{initial}}/U_{\text{final}}$. Since there is damping of the coherences and, more importantly, anharmonicity-induced dephasing in the system, the wave packet oscillations decay within a few cycles. The total energy of the trapped atoms, i.e., kinetic and potential energy, is closely related to the localization averaged over a period, $\overline{\Delta\xi^2(t)}$. On a longer time scale, $\overline{\Delta\xi^2(t)}$ exponentially approaches a steady state value which is close to the initial $\Delta\xi^2(0)$. This long-time increase of $\overline{\Delta\xi^2(t)}$, indicating heating, is clearly observed in Fig. 1: after compression $\overline{\Delta\xi^2(t)}$ approaches steady state with a time constant of $44 \pm 5 \mu\text{s}$ [11]. Under the same conditions the time constant of localization (cooling) of initially disordered atoms [7] was found to be $30 \pm 5 \mu\text{s}$. In 1D experiments (Fig. 2) and 1D quantum Monte Carlo wave function simulations (QMCWF) [12], the difference between heating and

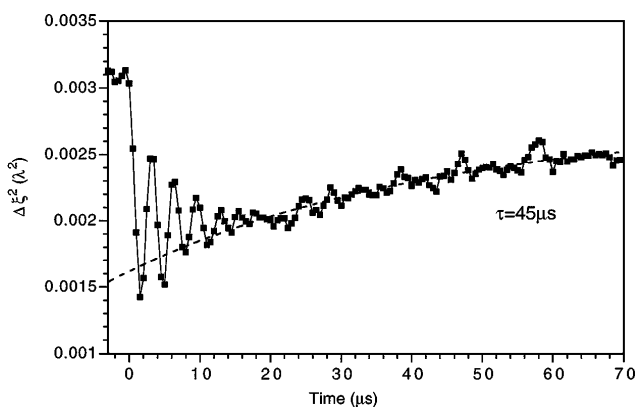


FIG. 2. Wave packet oscillations in a 1D lin \perp lin lattice induced by a sudden increase of the potential depth from $U_0 = 400E_R$ to $U_0 = 1850E_R$ at $t = 0$. The lattice detuning $\delta = -5\Gamma$. The long-term heating is best fitted with a time constant of $45 \mu\text{s}$ (dashed line), much longer than the localization time constant of $6 \mu\text{s}$ estimated for $U_0 = 1850E_R$ [7].

cooling times is much more dramatic, with heating a factor of 7 slower than cooling for the parameters of Fig. 2. The reasons for this difference between heating and cooling rates are still under investigation. It may be in part due to the Lamb-Dicke effect, which reduces inelastic photon scattering of well localized atoms by a factor of $k^2 \Delta\xi^2$.

In 1D the wave packet oscillations persist for more cycles, presumably due to smaller anharmonicity in our 1D potential wells compared to the 3D wells. In the typical 1D example shown in Fig. 2, we identify five oscillations, compared to three in the typical 3D case displayed in Fig. 1. In 1D we had less available laser power, limiting the maximum value of U . Thus, in order to obtain high transient compression $C = \sqrt{U_{\text{final}}/U_{\text{initial}}}$ we had to choose rather low values of U_{initial} , for which the steady state localization was slightly larger than usual. It may be that this accounts for the measured compression of only ≈ 1.5 , nevertheless producing a localization close to $\lambda/30$ ($\approx 30 \text{ nm}$). In many 1D results, as in the one shown in Fig. 2, there also appear to be additional oscillations after the initial oscillations have decayed away; these may be quantum revivals [13]. We do expect revivals in this system; in an anharmonic potential the dephasing of wave packet oscillations may be faster than the decay of individual vibrational coherences, and rephasing can produce revivals, which are observed in our 1D QMCWF calculations. Laser fluctuations tend to wash out the revivals, but we hope that experimental improvements will allow more detailed studies. We do not see revivals in 3D, presumably due to the more complicated vibrational spectrum in our anisotropic 3D lattice.

We extracted the frequency and the decay time of breathing-mode, wave packet oscillations by fitting data like those shown in Figs. 1 and 2 with functions $\Delta\xi^2(t) = \alpha \exp(-t/\tau) \cos(\omega t + \phi) + \beta \exp(-t/\tau_{\text{long}}) + \gamma$, for $0 < t < T_{\text{max}}$, all parameters being fitted. T_{max} is the time when the oscillations almost disappear. Since the fit results for ω and τ are mostly determined by a few initial oscillations, the value chosen for T_{max} influences the fit results only at the few percent level [14]. Fit values for the oscillation frequencies $\omega/2\pi$ are plotted in Fig. 3 versus the diabatic potential depth U_0 after the switching; $U_0 = (\hbar|\delta|/2)[\ln(1+s) - \ln(1+(1/45)s)]$. Here, the saturation parameter $s = 2\Omega^2/(\Gamma^2 + 4\delta^2)$, with the Rabi frequency Ω being for the strongest transition, at the lattice sites, and δ is the detuning. The uncertainties in U_0 shown in Fig. 3 (and Fig. 4) are due to intensity fluctuations; uncertainties in ω and τ are statistical fit estimates. In agreement with a harmonic model of the potential wells in both the 1D and the 3D experiments, the frequency is proportional to $\sqrt{U_0}$. However, the measured frequencies are only $86\% \pm 5\%$ in 1D and $68\% \pm 5\%$ in 3D of the values obtained using a harmonic well having the same curvature as our actual wells at the bottom. We observed a similar deviation when analyzing the sidebands

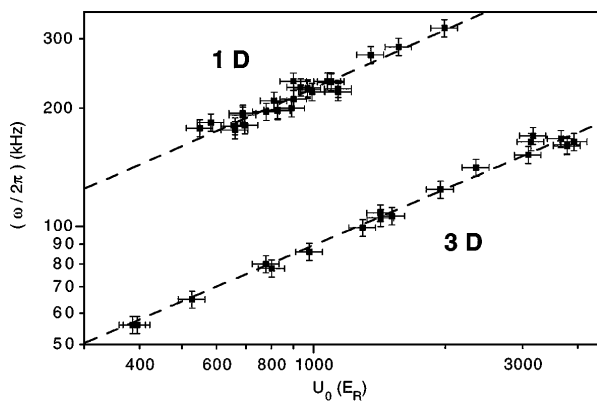


FIG. 3. Oscillation frequencies of the observed breathing-mode wave packet motion in 1D and 3D as a function of the final potential depth U_0 for detunings between $\delta = -2\Gamma$ to -15Γ . The dashed fit functions are $7.62 \text{ kHz} (U_0/E_R)^{0.49}$ in 1D, and $3.32 \text{ kHz} (U_0/E_R)^{0.48}$ in 3D.

in the spontaneous emission spectrum of atoms trapped in a lattice [9]. Our calculations of the 1D band structure show that the frequency reduction is due to the anharmonicity of the lattice potential. Since the energy of the atoms scales with the potential depth, and the shape of the potential is invariant, the anharmonicity-shifted frequency varies, like the harmonic frequency, as $\sqrt{U_0}$. In 3D the anharmonicity-induced frequency shift is approximately twice as large as in 1D. The frequency shifts observed in the present work are larger than those observed in [9] by amounts of 2% and 8% of the respective harmonic frequencies. This difference is not significant considering our experimental uncertainty of 5%, both here and in [9], which is primarily due to uncertainty in the lattice intensity.

Figure 4 shows fit values for the oscillation decay times τ . If the anharmonicity was the predominant cause of the decay of the wave packet oscillations, we would expect τ^{-1} to be proportional to $\sqrt{U_0}$ (for the same reason the anharmonicity-shifted frequency scales as $\sqrt{U_0}$). The fit in Fig. 4 shows that the 3D results below $U_0 = 3000E_R$ are consistent with such an anharmonicity-dominated decay. Above $U_0 = 3000E_R$ the lifetime τ is actually longer than expected from the inverse square-root dependence. In 1D, we do not find a clear dependence of τ on U_0 at all. For $\delta = -5\Gamma$ τ does not decrease for large U_0 , as also observed in 3D. We have no simple physical explanation for the unexpectedly long lifetimes at large U_0 , but we also see them in 1D QMCWF simulations. If we vary δ while keeping U_0 constant, we expect the anharmonicity to be unchanged, while the damping changes due to the changing photon scattering rate. Figure 4 suggests a detuning dependence of τ in 1D (similar to 1D QMCWF simulations), although not in 3D, presumably due to the larger 3D anharmonicity.

The Monte Carlo simulations show that the uncertainty product $\sqrt{\Delta\xi^2\Delta p^2}$ is approximately conserved during the oscillations. The reduction of the spread in one

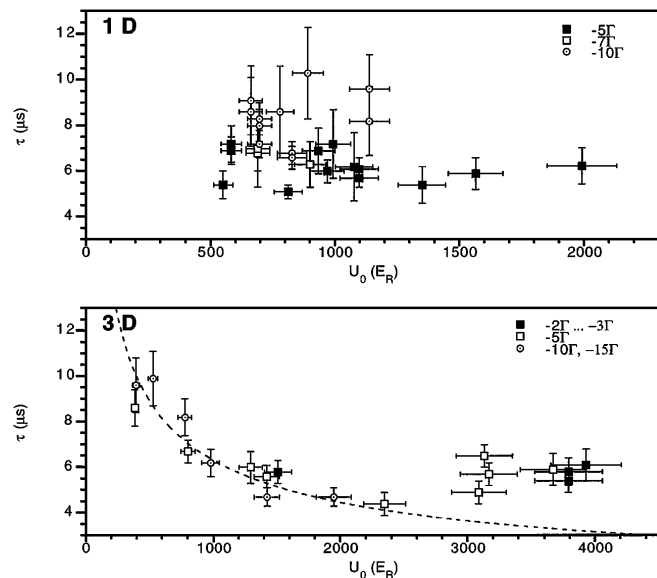


FIG. 4. Lifetimes τ of the breathing-mode wave packet motion in 1D and 3D as a function of the potential depth U_0 for the indicated values of the detuning δ . The 3D panel contains a fit consistent with anharmonicity-induced decay only.

conjugate variable at the expense of the other is similar to the case of squeezed states of light [15]. However, given the large spread of the initial wave packet and our limited compression, the spreads of momentum and position do not drop below those of the ground vibrational state, the standard quantum limit (SQL). In order to reach the SQL, one might consider switching to much deeper potentials with sufficiently large detuning to avoid saturation.

As an alternative way to obtain spatial localization below that in steady state, we studied parametrically driven atoms in our 3D lattice. After cooling the atoms in steady state, the lattice intensity is sinusoidally modulated with a frequency ν and peak-to-peak modulation depth M . After about thirty modulation periods, we measure the Bragg reflectivity as a function of the modulation phase Φ (measured with respect to an intensity maximum) at which the lattice is turned off. From the data we obtain $\Delta\xi^2(\Phi)$ with parameters ν and M , as shown in Fig. 5(a). In general, $\Delta\xi^2(\Phi)$ can be well fitted by a sinusoid, yielding a phase lag Θ , and an amplitude A . In Fig. 5(b) we show $\Theta(\nu)$ and $A(\nu)$ for a fixed M and specific lattice parameters. Maximum amplitude A of the wave packet oscillation is observed at a frequency ν equal to the breathing-mode frequency in the unmodulated lattice. The phase lag $\Theta \approx -\pi/2$ for maximum A , as expected for on-resonance drive. The large width of $A(\nu)$ corresponds to a time constant even shorter than those seen in Figs. 1, 3, and 4 in 3D.

Figure 5(a) shows that while there is some compression below the steady state, parametric driving increases the time averaged value of $\Delta\xi^2$ by an amount of about 2/3 of the modulation amplitude A . This leads to compression

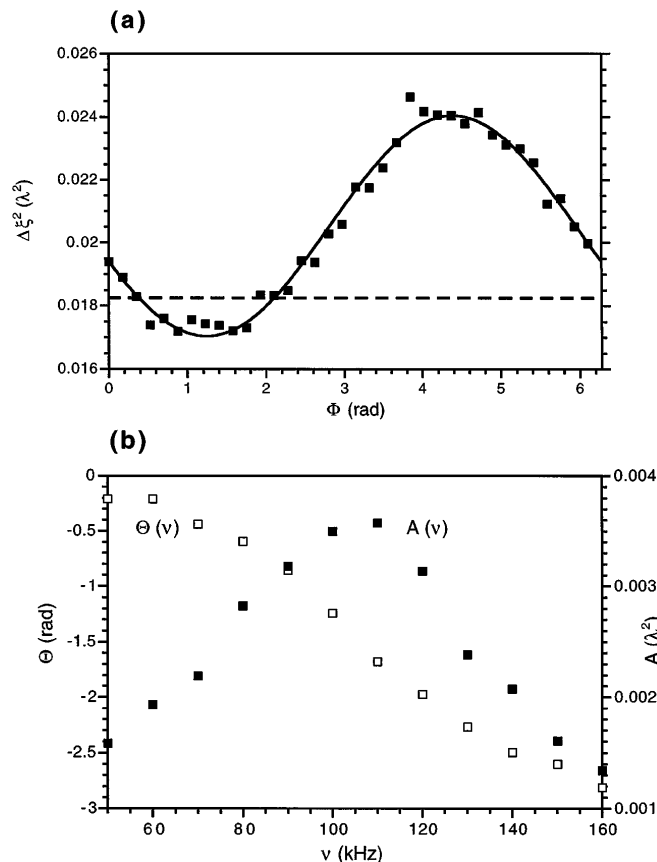


FIG. 5. (a) Phase-dependent localization $\Delta\xi^2(\Phi)$ and sinusoidal fit for a 3D optical lattice parametrically driven by an intensity modulation with frequency $\nu = 100$ kHz and peak-to-peak modulation depth $M = 25\%$. For the employed mean potential depth, $U_0 = 1430E_R$, and detuning $\delta = -5\Gamma$ this case is close to resonance. The dashed horizontal line shows the steady state value of $\Delta\xi^2$. (b) Amplitude A and phase lag Θ of oscillations in the localization $\Delta\xi^2$, deduced from fits to data analogous to (a) taken for different frequencies ν .

that is small when compared with the result obtained with the sudden-compression technique.

In this work breathing-mode wave packet motion of atoms localized in optical lattices has been studied using sudden-switching and parametric-drive techniques. The observed oscillation frequencies of the wave packets are in agreement with previous results and with Monte Carlo calculations. The heating rates after compression (Figs. 1 and 2), the lifetimes of the oscillations (Fig. 4), and the width of the observed resonance curves [Fig. 5(b)] still await a full understanding. The sudden-switching technique could be useful for studies requiring atoms with sub-steady-state localization. Using sudden switching, we obtained spatial compression factors of up to ≈ 2 . Higher compression factors should be readily achievable with more laser power. It should even be possible to reach position spreads below the width of the ground state wave function, thus entering the regime of quantum squeezed states. Applications may be designed such that they take advantage of the first collapse of the atomic

distribution after the switching event. Using the higher transient Bragg reflectivity, it might be easier to observe photonic bandgaps in optical lattices [16]. The technique can also be implemented in an environment where an atomic beam traverses a 1D or 2D optical lattice (lattice beams orthogonal to the atomic beam) with a tailored intensity profile. In the frame of reference of the atoms, the lattice intensity gradient in the atomic beam direction causes a temporal intensity change which can be designed such that sudden compression is obtained. A possible application of such a technique is the deposition of spatially compressed structures onto a substrate [17].

This work was partially supported by the U.S. Office of Naval Research and by NSF Grant No. PHY-9312572. G. Birkl and G. Raithel acknowledge support by the Alexander-von-Humboldt Foundation.

*Present address: Institut für Quantenoptik, Universität Hannover, Welfengarten 1, D-30167, Hannover, Germany.

- [1] P. Verkerk, B. Lounis, C. Salomon, C. Cohen-Tannoudji, J.-Y. Couetois, and G. Grynberg, *Phys. Rev. Lett.* **68**, 3861 (1992).
- [2] P. S. Jessen *et al.*, *Phys. Rev. Lett.* **69**, 49 (1992).
- [3] A. Hemmerich and T. W. Hänsch, *Phys. Rev. Lett.* **70**, 410 (1993).
- [4] M. B. Dahan, E. Peik, J. Reichl, Y. Castin, and C. Salomon, *Phys. Rev. Lett.* **76**, 4508 (1996).
- [5] S. R. Wilkinson, C. F. Bharucha, K. W. Madison, Qian Niu, and M. G. Raizen, *Phys. Rev. Lett.* **76**, 4512 (1996); Qian Niu, Xian-Geng Zhao, G. A. Georgakis, and M. G. Raizen, *Phys. Rev. Lett.* **76**, 4504 (1996).
- [6] G. Birkl, M. Gatzke, I. H. Deutsch, S. L. Rolston, and W. D. Phillips, *Phys. Rev. Lett.* **75**, 2823 (1995).
- [7] G. Raithel, G. Birkl, A. Kastberg, W. D. Phillips, and S. L. Rolston, *Phys. Rev. Lett.* **78**, 630 (1997).
- [8] M. Weidemüller, A. Hemmerich, A. Görlitz, T. Esslinger, and T. Hänsch, *Phys. Rev. Lett.* **75**, 4583 (1995).
- [9] M. Gatzke, G. Birkl, P. Jessen, A. Kastberg, S. L. Rolston, and W. D. Phillips, *Phys. Rev. A* (to be published).
- [10] S. Marksteiner, R. Walser, P. Marte, and P. Zoller, *Appl. Phys. B* **60**, 145 (1995).
- [11] In this paper all quoted uncertainties are combined standard uncertainties (estimated one standard deviation).
- [12] J. Dalibard, Y. Castin, and K. Mølmer, *Phys. Rev. Lett.* **68**, 580 (1992).
- [13] J. H. Eberly, N. B. Narozhny, and J. J. Sanchez-Mondragon, *Phys. Rev. Lett.* **44**, 1323 (1980).
- [14] We did not fit the entire curve because the existence of revivals is not included in our fit function.
- [15] See, e.g., D. F. Walls and G. J. Milburn, *Quantum Optics* (Springer, Berlin, 1994).
- [16] I. H. Deutsch, R. J. C. Spreeuw, S. L. Rolston, and W. D. Phillips, *Phys. Rev. A* **52**, 1394 (1995).
- [17] G. Timp, R. Behringer, D. Tenneant, J. Cunningham, M. Prentiss, and K. Berggren, *Phys. Rev. Lett.* **69**, 1636 (1992); J. J. McClelland, R. E. Scholten, and E. C. Palm, *Science* **262**, 3231 (1993).